

## Synthesis of exfoliated polystyrene/SWY-Na nanocomposite by emulsion polymerization using a chloride of cétylpyridinium and dielectric proprieties

H. Ezzaier, Regis Guegan, Amel Jmayai, Marwa Glid, Atef Riahi, A. Ben Haj Amara, Fabric Muller, and H. Ben Rhaïem

Laboratoire de physique des matériaux lamellaires et nanomatériaux hybrides,  
Institut de la science de la terre d'Orléans,  
Université d'Orléans, France

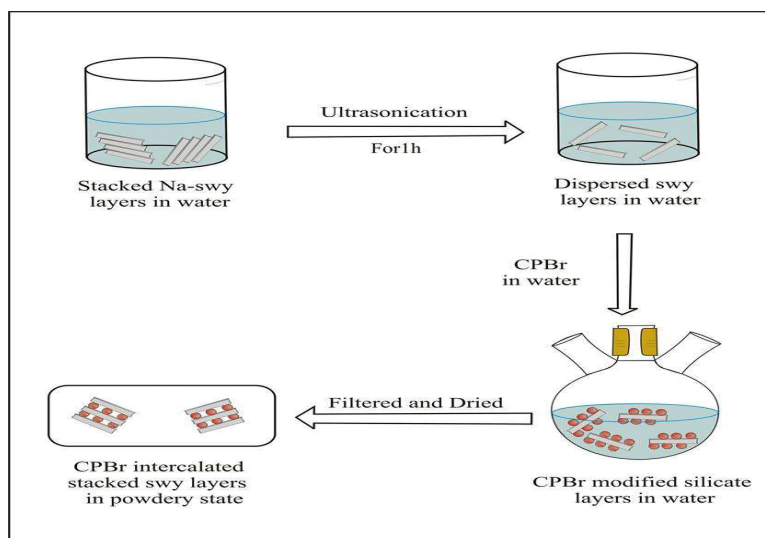
Copyright © 2014 ISSR Journals. This is an open access article distributed under the **Creative Commons Attribution License**, which permits unrestricted use, distribution, and reproduction in any medium, provided the original work is properly cited.

**ABSTRACT:** Polymer nanocomposites of polystyrene matrix containing 5 wt % of organoswy were prepared using the solution method with sonication 23 hours. CPBr is used to modify the SWY clay after suturing with surface with  $\text{Na}^+$ . Polystyrene was synthesized through solution polymerization in the presence of potassium persulfate (KPS) as an initiator. The synthesized PS/oswy were characterized by XRD, FTIR, SEM methods. Frequency dependent complex dielectric function, loss tangent spectra of PS and PS/swy nanocomposites up to 5 wt %. The nanocomposite materials with low dielectric constant and loss tang compared to the pure polystyrene were obtained. The dielectric constant increase with the increase of temperatures.

**KEYWORDS:** clay, swy, oswy, CEC, RX, SEM, IR, Dielectric.

### 1 INTRODUCTION

Polymer-layered silicate nanocomposites have become effective alternatives to conventional composites in many applications. Nanocomposites, such as polymer-layered silicate nanocomposites, have a least one characteristic dimension in the order of the nanometer. In general, two types of clay nanocomposites can be obtained intercalates and exfoliates [3,4, 5]. Intercalated are obtained when single polymer chain is located between clay layer spacing while attractive forces between the layers keep these in a regular spaced stacks.



Polystyrene (PS) is a commercialized and mass productive polymer. Hence, continuing research efforts have been devoted to the development of polystyrene/montmorillonite (PS/MMT) nanocomposites. Various methods based on simple mechanical mixing, bulk polymerization, solution polymerization and emulsion polymerization have been employed.

So far the majority of PS/MMT nanocomposites prepared via emulsion polymerization showed an intercalated morphology. In this paper, we use a novel zwitterion amino acid to modify the clay, and PS/MMT composite is synthesized via emulsion polymerization in the presence of the modified clay. This approach is proved to be effective for the preparation of water-borne exfoliated polymer/clay nanocomposites. For comparison, emulsion polymerization in the presence of cetyltrimethylammonium bromide-modified MMT or pristine sodium montmorillonite are also studied.

Polymer-clay nanocomposite materials, in which nanometer-thick layers of clay dispersed in polymers, are generally stiffer, stronger, and tougher than normal polymeric materials and can be potentially useful in a variety of applications. These polymer-clay nanocomposites can be prepared in several ways, namely by intercalation where polymer chains are sandwiched in between silicate layers and by exfoliation where separated, individual silicate layers are more or less uniformly dispersed in the polymer matrix. However, exfoliation and orientation of the clay platelets in the polymer matrix is not optimized for the approaches currently used to prepare polymer-clay nanocomposites. The objective of this work is to prepare anisotropic polymer-clay nanocomposite particles with exfoliated clay platelets encapsulated inside latex particles in order to improve the exfoliation and orientation of the clay platelets in the final polymeric film. In our present study, we report for the first time a simple in situ preparation and characterization of an exfoliated polystyrene clay nanocomposites site with low dielectric constant, the microstructure of nanocomposites were determined by X-ray Diffraction (XRD) and Scanning Electron Microscope (TEM) and their dielectric proprieties were also investigated.

## **2 EXPERIMENTAL**

### **2.1 MATERIALS**

Styrene monomers sodium dodcylsulfate (SDS, Aldrich, 99%) and the initiator, potassium persulfate (Kps, Aldrich, 98%), Raw Wyoming was collected from Bir El Hfei (Gafsa), the chemical composition was determined using X-ray florescence (XRF).

### **2.2 MEASUREMENTS**

BET surface area and pore volumes of adsorbent were measured using the physical adsorption of nitrogen by quantachrome Autosorb-1 instruments.

The cationic exchange capacity of CEC was determined using the cooper ethylene diamine (EDA)<sub>2</sub> Cu Cl<sub>2</sub>) complex.

The X-ray diffraction patterns of the polystyrene PS were measured using the CuK<sub>α1</sub> (1,5406Å) radiation in the range of 2θ=10-70°, with a step size of 0.02°.

The infrared spectroscopic absorption data were obtained with a Fourier TransformInfrared spectrometer with an attenuated total reflectance accessory (FTIR-ATR).

Finally the electrical measurements of dielectric constant, dielectric loss and impedance parameters Z'' and Z' were made over a wide range of temperatures (40°C-200°C) with cooling rate of 10°C and a stabilization time of 10 min between consecutive measurements and a frequency of (10 Hz --13 MHz), by means of a Hewlett Packard HP 4192A impedance analyzer.

### **2.3 PREPARATION METHODS**

#### **2.3.1 SYNTHESIES OF POLYSTYRENE**

Polystyrene were prepared in batch emulsion polymerization at 80°C from styrene (Aldrich, 99%), in 200 ml of H<sub>2</sub>O the surfactant, sodium dodcyl sulfate (SDS, Aldrich, 99%) and the initiator, potassium persulfate (Kps, Aldrich, 98%). Removing SDS and conterions from the suspension from the experiments,

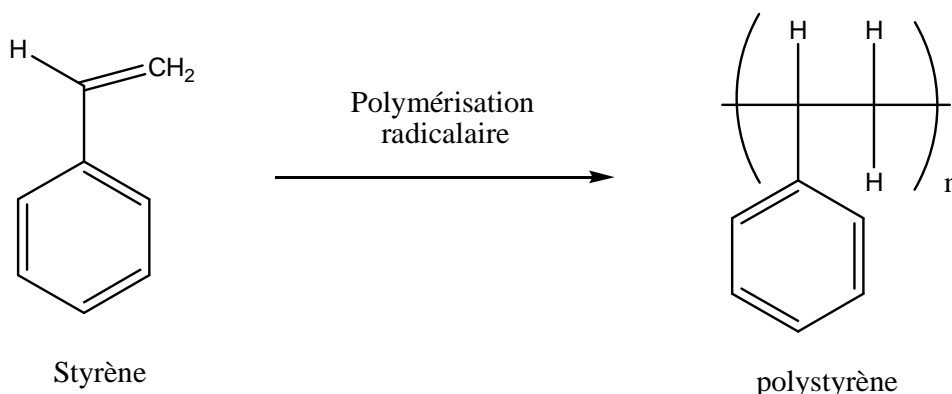


Fig. 1. 1. Method of Synthesis of polystyrene.

### 2.3.2 WASHING AND SATURATION OF SWY

To prepare the suspension, 31 ml of distilled water was added to 150 g of SWY and shaken for 24h. The suspension was allowed to sit for 30 min. Distilled water was added to the separated swy suspension. After, the swy suspension was separated and saturated by shaking with 0.5 mol/L of NaCl solution for 24 h. This step was repeated five times. The sediments were washed with distilled water to remove excess salt. This was confirmed by a negative chloride ion test using  $\text{AgNO}_3$ . The organoswy were prepared by drop wise addition of 0,1 M aqueous solutions of CPBr to a 0.5 % aqueous suspension of the Na – SWY, it was stirred for 24 h. The complexes were centrifuged and washed several times with distilled water until the absence of chloride in the filtrate. The organoswy was dried in hot air dried.

### 2.3.3 PS/oswy

Ten percent of the weight of organoswy was added to 20 ml of toluene. The suspension was stirred magnetically for 1h and sonicated for 1h before PS (2g) was added. The resulting mixture was magnetically stirred for 1h and sonicated for 2h.

## 3 RESULTS AND DISCUSSION

### 3.1 CHEMICAL COMPOSITION OF SWY

The chemical composition of swy as well as surface area and organoswy are shown in Table 1. BET surface area of swy and organoswy was measured using the physical adsorption of nitrogen by quantachrome Autosorb-1 instruments.

Table.1. the chemical composition of raw swy.

Constituent	Percentage (%)	Cation exchange	Adsorbent	Specific surface area
$\text{SiO}_2$	52,98	92 meq/100g	swy	27
$\text{Al}_2\text{O}_3$	16,32		oswy	2.3
$\text{Fe}_2\text{O}_3$	7,26			
CaO	2,52			
MgO	3,86			
$\text{Na}_2\text{O}$	0,5			
$\text{K}_2\text{O}$	0,5			
Loss of ignition	14,20			

### 3.2 XRD

XRD analysis of swy and organoswy shows information of interlayer spacing of the clay layers (Fig.1). After the cation exchange with CPBr, the  $d_{001}$  spacing was expanded. This increase of d spacing provides evidence to support the exchange of the interlayer by  $\text{CPBr}^+$ . The results of basal spacing of each synthesized organo-swy and swy are given in Table1.

Table. 2. XRD Results of swy and organo-swy (1 CEC, 2 CEC and 3 CEC).

samples	swy	1CEC	2 CEC	3 CEC
$d_{001}$	12.5	40.07 Å	39.09Å°	38.41Å°
$2\theta(^{\circ})$	5	1.8	5.7	1.5

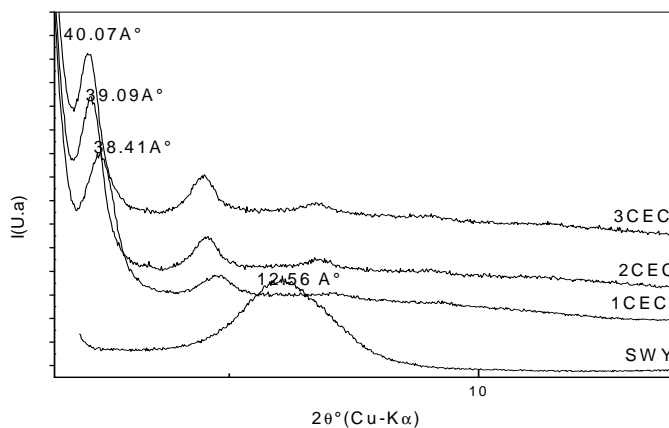


Fig.1. X-ray powder diffraction patterns of swy and oswy equivalent to 1, 2 and 3 times the CEC.

### 3.3 FTIR

The infrared absorption spectra (FT-IR) of swy and organoswy were recorded in the region from 400-4000 $\text{cm}^{-1}$ . For the swy spectrum, the absorption band at 3645  $\text{cm}^{-1}$  is because of the stretching vibrations of structures OH groups coordinated to AL-AL pairs the complex broad band at approximately, and the bands are related to Al-O-Si, Si-O-Si deformations. Adsorbed molecules of water result in abroad bad at 3403  $\text{cm}^{-1}$  which corresponds to the H<sub>2</sub>O stretching vibrations was at 1639 $\text{cm}^{-1}$ [6]. The additional peaks at 1425 and 1467  $\text{cm}^{-1}$  in organoclay, which are absent in swy, indicate the presence of C-N vibrations intertiary amines. This observation clearly indicates that the surface modification of swy is achieved by surfactant.

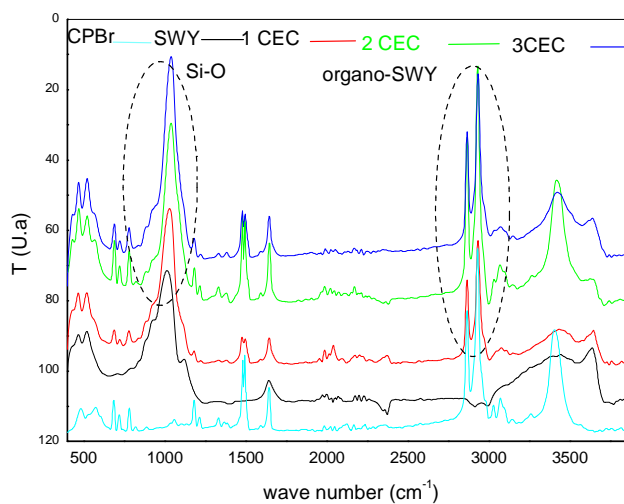


Fig.2. FTIR patterns of swy and oswy equivalent to 1, 2 and 3 times the CEC

### 3.4 SEM

Scanning electron microscopy (SEM) shows some significant changes on the surface of the organoclay oswy (1 CEC, 2 CEC and 3 CEC) Fig.4. The Na-treated smectites appears, some aggregated and some massive. However the clay treated with organic surfactants (Fig.3.b, c and d) shows slightly non aggregated morphology, and severely curled or crumpled edges. The organoclay particules (oswy) are relatively separated (Fig.4.b, c and d) it seems that the replacement of the inorganic interlayer cations and their hydratation with CPBr<sup>+</sup>

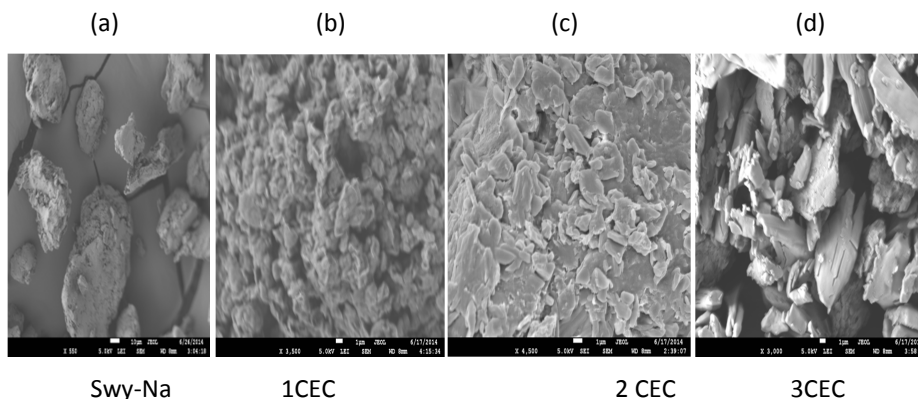


Fig.3. SEM images of OSWY

Spherulite-looking crystals with beautiful impinged boundaries were observed in PS/organo-MMT after 1 h of sonication time compared to PS. Good dispersion of this percentage of MMT throughout the PS matrix under sonication could be led to a nucleation effect and increase the percentage of crystallinity. It is result strongly agrees with the XRD results.

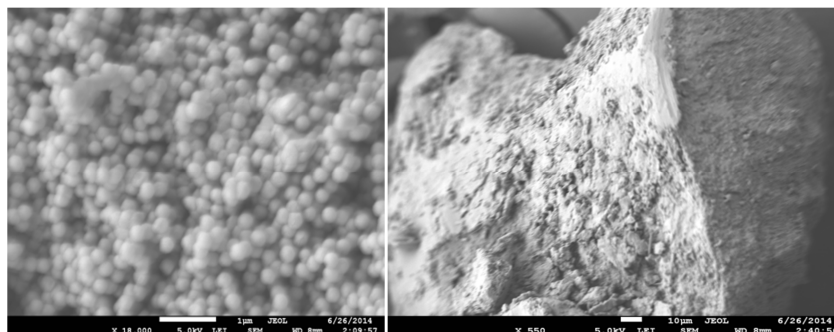
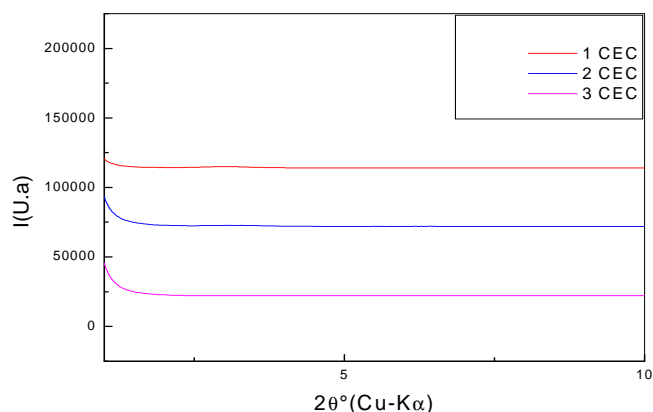


Fig.4. SEM images of PS/OSWY

### 3.5 XRD

XRD technique is widely used to investigate the dispersion degree of swy in matrices. Intercalated and/ or exfoliated polymer/oswy nanocomposites can be classified based on displacing of the peak in terms of the gallery height of swy. The characteristic peak of the organoswy (at  $2\theta=2^\circ$ ) was disappeared in the nanocomposites. These XRD indicate to the fact that the ordered structure of the clay was destroyed, resulting a well exfoliated morphology in the PS/oswy nanocomposites [8].



**Fig. 5. XRD patterns of organo-swy**

### 3.6 FTIR

The infrared of PS features bands at 3066, 3025, 2922, 2851, 1666-1945, 1491-1599, 1188-1368, 1026, 698-756, and 543 $\text{cm}^{-1}$  [11, 9]. The infrared spectra (FT-IR) of PS /organoswy nanocomposites were recorded in the region from 400 $\text{cm}^{-1}$  - 400 $\text{cm}^{-1}$  as shown in figure.7. In these spectra, all PS bands appeared in these spectra with slight shifting. New bands appeared in the regions of 3625, 1027, and 466 $\text{cm}^{-1}$  were attributed to OH stretching of structural hydroxyl groups (AL-OH) and bending vibrations of organoswy and were indicating the existence of organoswy and were indicating the existence of organoswy in the PS matrix where the polymer chain was inserted between the layers of the organoswy by secondary valence force (Fig .6).

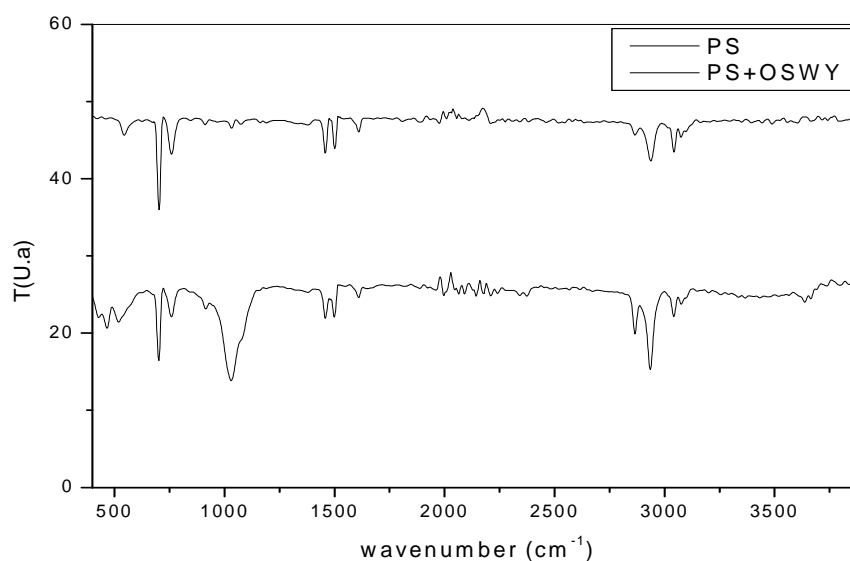


**Fig.6. FTIR patterns of PS, PS/oswy**

Table. I.1. Positions and assignments of the IR vibration bands of PS.

Wavenumber ( $cm^{-1}$ )	Assignment
3066 et 3026	Stretching vibration of aromatic C-H
2922et2851	Stretching vibration of aliphatic C-H
1666-1945	Overtan and combunation bands (monosubstituted aromatic)
1491	Stretching vibration of aromatic C=C
1188-1368	Stretching vibration of aliphatic C-H
1026	Stretching vibration of aliphatic C-H
698-756, 543	Stretching vibration of aromatic C-H

### 3.7 DIELECTRIC RELAXATION SPECTROSCOPY.

#### 3.7.1 THE COMPLEX DIELECTRIC FUNCTION SPECTRA

The real part (permittivity)  $\epsilon'$  and imaginary part (dielectric loss)  $\epsilon''$  of the complex relative dielectric function can be seen in Fig.8 the dielectric constant of pure PS and PS/organoclay nanocomposites with different temperatures. The reduction in the dielectric constant of the PS can be explained a complicated polarization. It is clear from this figure that  $\epsilon$  decrease by increasing organoclay concentrations. At low frequencies and higher while at higher frequencies the rate becomes very slow. An explication for this is that at low frequencies, the dipole movements and charge carriers can freely move within the material while at higher frequencies dipole and charge carriers become to follow variations of the applied electric field resulting in a dependence of tangent loss of nanocomposites [19, 20, 21, 23, 24].

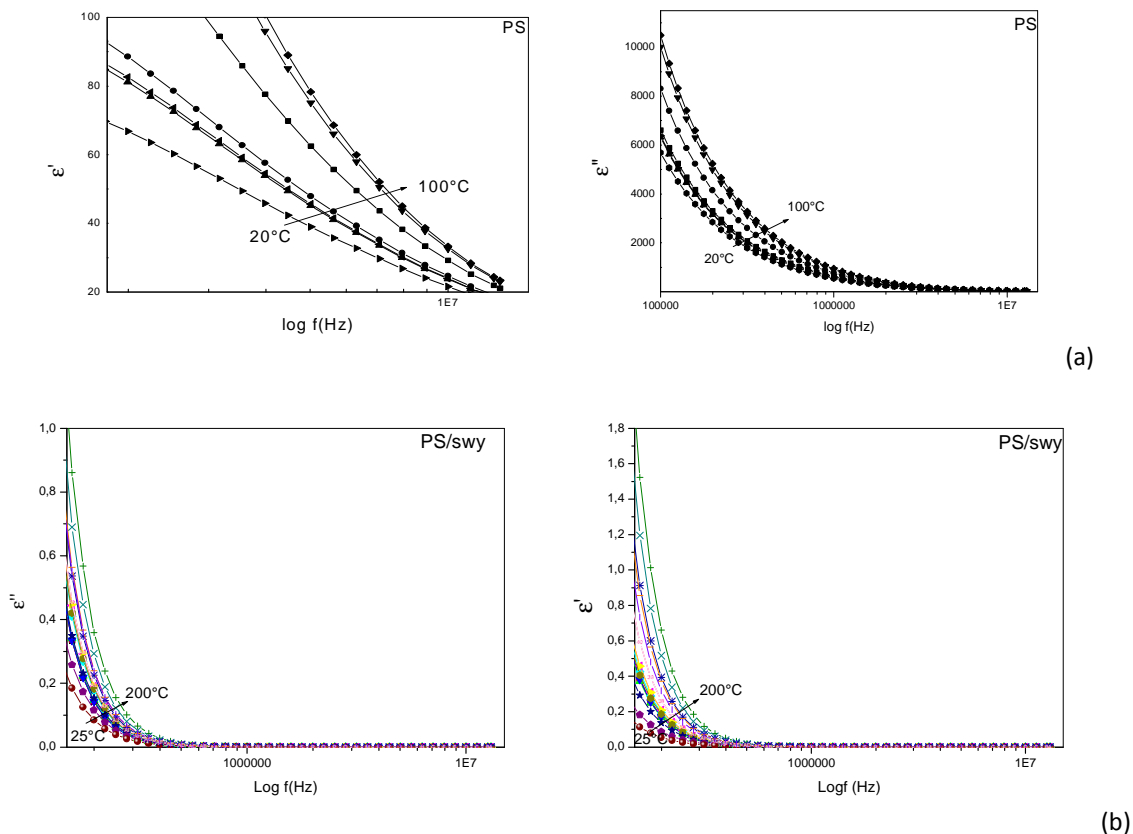


Figure.7. the dielectric constant of polystyrene (a) and nanocomposites (b) at various temperatures and frequencies

### 3.7.2 DIELECTRIC LOSS TANGENT SPECTRA

The dielectric loss  $\delta$  of polystyrene and nanocomposites (PS/organoclay) are shown in Fig.9, it indicate that the tang loss of pure polystyrene and nanocomposites increased slightly up to 1000 Hz then rapidly decreased with frequency range suggest the existence of one or more of the following processes: (i) electrode polarization, (ii) interfacial polarization and (iii) conductivity phenomenon . This is the case in polymer matrix-inorganic filler composites due to the accumulation of mobile charges at the interface of the constituents. The Tangent losses for pure polystyrene and nanocomposites (PS/swy) are due to the dipolar relaxations at this frequency for PS/swy are readily explained by interfacial polarization between the interface of clay mineral and polymer matrix. This why interfacial polarization appears at low frequencies in the nanocomposites. This maximum tangent loss of the samples was observed at low frequencies than at high frequencies [16, 17, 18, 23], the decrease in dielectric losses is due to the intercalation and exfoliation of the clay layers.

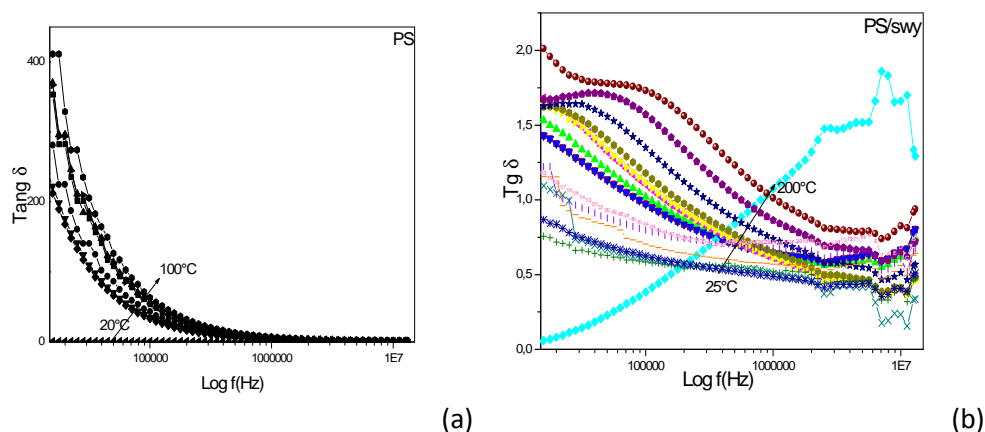


Figure.7. the dielectric loss of polystyrene (a) and nanocomposites (b) at various temperatures and frequencies

## 4 CONCLUSION

In conclusion the synthesized PS/oswy was characterized by XRD, FTIR, SEM methods. The results showed that the PS/swy nanocomposites have better dielectric proprieties in our experimental conditions. DRX, SEM, FTIR confirms the dispersion of nanometer silicate layers in the PS. The dielectric constants decreased with the increase of the clay content. The materials with lower dielectric constant than pure PS which can be used in particularly electric-electronic industry were obtained.



## REFERENCES

- [1] P. Baskaralingam, M. Pulikesi, D. Elango, V. Ramamurthi, S. Sivanesan, Adsorption of acid dye onto organobentonite, *Journal of Hazardous Materials B128* (2006) 138–144.
- [2] H. Freundlich, *hem.*, *Z. Phys. C A57* (1906) 385.
- [3] M. Alexandre, P. Dubois, *Mater. Sci. Eng.* 28 (2000) 1–63.
- [4] M. Zanetti, S. Lomakin, G. Camino, *Macromol. Mater. Eng.* 279 (2000) 1–9.
- [5] Tamer A. Elbokl, Christian Detellier, *Physics and Chemistry of Solids* 67 (2006) 950–955.
- [6] Daniela Placha, Grażyna Simha Martynkova, Mark H. Rummeli, Preparation of organovermiculites using HDTMA: Structure and sorptive properties using naphthalene, *Journal of Colloid and Interface Science* 327 (2008) 341–347.
- [7] Supratim Suin, Sandip Maiti, Nilesh K. Shrivastava, B.B. Khatua, Mechanically improved and optically transparent polycarbonate/clay nanocomposites using phosphonium modified organoclay, *J. Materials and Design* 54 (2014) 553–563.
- [8] Choi, Y. S.; Ham, H. T.; Chung, I. J. Polymer/silicate nanocomposites synthesized with potassium persulfate at room temperature: polymerization mechanism, characterization, and mechanical properties of the nanocomposites. *Polymer* 2003, 44, 8147–8154.
- [9] Tamer A. Elbokl, Christian Detellier; Aluminosilicate nanohybrid materials. Intercalation of polystyrene in kaolinite; *Journal of Physics and Chemistry of Solids* 2006, 67, 950–955.
- [10] Hui Yin, Li Mañ, Mengyu Gan, Zhitao Li, Xiaoyu Shen, Shuang Xie, Jun Zhang, Jiyue Zheng, Fenfang Xu, Jinlong Hu, Jun Yan; Preparation and properties of poly(2,3 dimethylaniline)/organic-kaolinite nanocomposites via in situ intercalative polymerization; *Composites Science and Technology* 94 (2014) 139–146.
- [11] Yanfeng Li \*, Bo Zhang, Xiaobing Pan Preparation and characterization of PMMA-kaolinite intercalation composites *Composites Science and Technology* 68 (2008) 1954–1961.
- [12] Reidar Lund, Sandra Plaza-García, Angel Alegría, Juan Colmenero, Jonathan Janoski d, Sumana Roy Chowdhury d, Roderic P. Quirk. Dielectric relaxation of various end-functionalized polystyrenes: Plastification effects versus specific dynamics; *Journal of Non-Crystalline Solids* 356 (2010) 676–679.
- [13] Yei DR, Kuo SW, Su YC, Chang FC. Enhanced thermal properties of P nanocomposites formed from inorganic POSS-treated montmorillonite. *Polymer* 2004;45:2633–40.
- [14] Kuo SW, Chang FC. POSS related polymer nanocomposites. *ProgPolym Sci* 2011;36:1649–96.
- [15] Noh MH, Jang LW, Lee DC. Intercalation of styrene-acrylonitrile copolymer in layered silicate by emulsion polymerization. *J Appl Polym Sci* 1999;74:179–88.
- [16] Esra Evrim Yalçinkaya, Mehmet Balcan, Çetin Güler Synthesis, characterization and dielectric properties of polynorbadiene/clay nanocomposites by ROMP using intercalated Ruthenium catalyst. *J. Materials Chemistry and Physics* 143 (2013) 380e386.
- [17] Pradip Thakur, Arpan Kool, Biswajoy Bagchi, Sukhen Das, Papiya Nandy, Enhancement of  $\beta$  phase crystallization and dielectric behavior of kaolinite/halloysite modified poly(vinylidene fluoride) thin films, *J. Applied Clay Science* 99 (2014) 149–159.
- [18] R. Crétois, L. Delbreilh, E. Dargent a,d, N. Follain, L. Lebrun, J.M. Saiter, Dielectric relaxations in polyhydroxyalkanoates/organoclay Nanocomposites, *J. European Polymer Journal* 49 (2013) 3434–3444.
- [19] Do Hoon Kim, Kwang Soo Cho, Tetsu Mitsumata, Kyung Hyun Ahn, Seung Jong Lee. Microstructural evolution of electrically activated polypropylene/layered silicate nanocomposites investigated by in situ synchrotron wide-angle X-ray scattering and dielectric relaxation analysis, *J. Polymer* 47 (2006) 5938e5945.
- [20] R.J. Sengwa, Shobhna Choudhary, Sonu Sankhla; Dielectric properties of montmorillonite clay filled poly(vinyl alcohol)/poly(ethylene oxide) blend nanocomposites, *J. Composites Science and Technology* 70 (2010) 1621–1627.
- [21] Anthony J. Bur, Yu-Hsin Lee, Steven C. Roth, Paul R. Start, Measuring the extent of exfoliation in polymer/clay nanocomposites using real-time process monitoring methods, *J. Polymer* 46 (2005) 10908–10918.
- [22] M. Pluta, J.K. Jeszka, G. Boiteux, Polylactide/montmorillonite nanocomposites: Structure, dielectric, viscoelastic and thermal properties. *J. European Polymer Journal* 43 (2007) 2819–2835.
- [23] Kirt A. Page, Keiichiro Adachi, Dielectric relaxation in montmorillonite/ polymer nanocomposites. *J. Polymer* 47 (2006) 6406–6413.
- [24] Kensaku Sonoda, Merja Teirikangas, Jari Juuti, Yasuo Moriya, Heli Jantunen, Effect of surface modification on dielectric and magnetic properties of metal powder/polymer nanocomposites. *J. Journal of Magnetism and Magnetic Materials* 323 (2011) 2281–2286.